frontiers | Frontiers in Molecular Neuroscience

TYPE Brief Research Report
PUBLISHED 28 April 2023
DOI 10.3389/fnmol.2023.1161086

OPEN ACCESS

EDITED BY
Lilian Kisiswa,
Aarhus University, Denmark

REVIEWED BY
Luis R. Hernandez-Miranda,
Charité University Medicine Berlin, Germany
Antonio Gennaro Nicotera,
University of Messina, Italy

*CORRESPONDENCE
David F. Butler
✉ dfbutler@wustl.edu
Kathleen J. Millen
✉ kathleen.millen@seattlechildrens.org

†PRESENT ADDRESS
David F. Butler,
Division of Critical Care Medicine, Department of Pediatrics, Washington University School of Medicine, St. Louis, MO, United States

RECEIVED 07 February 2023
ACCEPTED 10 April 2023
PUBLISHED 28 April 2023

CITATION
Butler DF, Skibo J, Traudt CM and Millen KJ (2023) Neonatal subarachnoid hemorrhage disrupts multiple aspects of cerebellar development.
Front. Mol. Neurosci. 16:1161086.
doi: 10.3389/fnmol.2023.1161086

Neonatal subarachnoid hemorrhage disrupts multiple aspects of cerebellar development

David F. Butler[1*†], Jonathan Skibo[2], Christopher M. Traudt[3] and Kathleen J. Millen[2,4*]

[1]Division of Pediatric Critical Care, Seattle Children's Hospital, University of Washington, Seattle, WA, United States, [2]Center for Integrative Brain Research, Seattle Children's Research Institute, Seattle, WA, United States, [3]Salem Health Hospitals and Clinics, Salem, OR, United States, [4]Department of Pediatrics, University of Washington Medical School, Seattle, WA, United States

Over the past decade, survival rates for extremely low gestational age neonates (ELGANs; <28 weeks gestation) has markedly improved. Unfortunately, a significant proportion of ELGANs will suffer from neurodevelopmental dysfunction. Cerebellar hemorrhagic injury (CHI) has been increasingly recognized in the ELGANs population and may contribute to neurologic dysfunction; however, the underlying mechanisms are poorly understood. To address this gap in knowledge, we developed a novel model of early isolated posterior fossa subarachnoid hemorrhage (SAH) in neonatal mice and investigated both acute and long-term effects. Following SAH on postnatal day 6 (P6), we found significant decreased levels of proliferation with the external granular layer (EGL), thinning of the EGL, decreased Purkinje cell (PC) density, and increased Bergmann glial (BG) fiber crossings at P8. At P42, CHI resulted in decreased PC density, decreased molecular layer interneuron (MLI) density, and increased BG fiber crossings. Results from both Rotarod and inverted screen assays did not demonstrate significant effects on motor strength or learning at P35–38. Treatment with the anti-inflammatory drug Ketoprofen did not significantly alter our findings after CHI, suggesting that treatment of neuro-inflammation does not provide significant neuroprotection post CHI. Further studies are required to fully elucidate the mechanisms through which CHI disrupts cerebellar developmental programming in order to develop therapeutic strategies for neuroprotection in ELGANs.

KEYWORDS

cerebellar hemorrhage, cerebellar development, preterm brain injury, Purkinje cells, cerebellar granule cells

Introduction

Despite improvements in survival rates for extremely low gestational age neonates (ELGANs; <28 weeks gestation), ~50% of survivors go on to have significant neurodevelopmental dysfunction including cognitive, learning, and/or motor deficits. Many of these deficits do not seem to be explained by cerebral white matter injury and/or intraventricular hemorrhage, suggesting an alternate mechanism of injury (Nosarti et al., 2007; Limperopoulos et al., 2014). Recent data suggests that injury to the cerebellum contributes to neurodevelopmental deficits and that developmental disruption of the cerebellum has widespread effects on neurologic function (Haines et al., 2013; Dijkshoorn et al., 2020; Brossard-Racine and Limperopoulos, 2021; Spoto et al., 2021).

Between 20 and 40 weeks of gestation, cerebellar growth is vigorous, with the volume of the cerebellum increasing at least five-fold. This rapid growth is almost exclusively driven by massive proliferation of granule neuron progenitors in the external granule layer (EGL). These progenitors will then differentiate into cerebellar granule cells (GC) and migrate into to their final location beneath the developing Purkinje cells *via* fibers of Bergman Glial cells to form the internal granule cell layer (IGL) (Rakic, 1971; Abraham et al., 2001; Volpe, 2009; Consalez et al., 2020). As the cerebellum rapidly grows, the developing cerebellar circuitry is also undergoing rapid remodeling and maturation. Disruptions of this early circuitry alter long term cerebellar circuit maturity (Haldipur et al., 2011; Barron and Kim, 2020; van der Heijden and Sillitoe, 2021; van der Heijden et al., 2021) and deranged cerebro-cerebellar neuronal circuitry causing impaired cerebral development and profound neurologic dysfunction (Limperopoulos et al., 2010, 2014; Wang et al., 2014; D'Mello and Stoodley, 2015; Stoodley and Limperopoulos, 2016; Brossard-Racine and Limperopoulos, 2021).

Injury to the neonatal cerebellum has been increasingly recognized in the ELGANs population. Many factors, including nutritional deficits, infection, inflammation and glucocorticoid exposure can disrupt cerebellar development in preterm infants (Buddington et al., 2018; Iskusnykh et al., 2018, 2021; Gano and Barkovich, 2019; Chizhikov et al., 2020; Iskusnykh and Chizhikov, 2022). Cerebellar hemorrhagic injury (CHI) is a relatively frequent finding in preterm infants, and even more common in severely premature infants (Steggerda et al., 2009; Boswinkel et al., 2019; Villamor-Martinez et al., 2019). Radiologic evidence of cerebellar subarachnoid and parenchymal hemorrhages correlates with poor neurodevelopmental outcomes (Johnsen et al., 2005; Steggerda et al., 2009; Zayek et al., 2012; Matsufuji et al., 2017; Boswinkel et al., 2019; Brossard-Racine and Limperopoulos, 2021). Hemorrhage is also highly associated with cerebellar hypoplasia (Volpe, 2009; Aldinger et al., 2019; Gano and Barkovich, 2019; Scelsa et al., 2022). Additionally, documented fetal cerebellar hemorrhage has been associated with cerebellar hypoplasia and neurodevelopmental deficits in full term children (Poretti et al., 2008). Furthermore, cerebellar hypoplasia on MRI has been shown to be more predictive of neurodevelopmental deficits than supratentorial injuries such as intraventricular hemorrhage or white matter injury (Limperopoulos et al., 2007).

While hemorrhage has been associated with cerebellar hypoplasia, the underlying injury mechanism is not fully understood. Extravasated blood and/or blood components have been shown to be injurious to multiple cell populations in the developing cerebral cortex, including neurons, glia, and oligodendrocytes (Xue et al., 2003; Vinukonda et al., 2012). Lypophosphatidic acid (LPA), a component of serum, induces hydrocephalus when injected into the lateral ventricles of embryonic mice due to ependymal injury and progenitor delamination into the lateral ventricles (Yung et al., 2011). Additionally, hemosiderin deposition may contribute to increases in reactive oxygen species (Volpe, 2009). However, the cerebellar-specific literature is very limited. We previously reported that a rabbit model of cerebellar subarachnoid hemorrhage induced in neonatal rabbits *via* systemic glycerol administration is invalid since glycerol itself is toxic to cerebellar development even in the absence of hemorrhage (Traudt et al., 2014). One of the first mouse models of neonatal cerebellar hemorrhage involved intraventricular injection of bacterial collagenase into the fourth ventricle of early post-natal mice, when maximal EGL proliferation occurs in this species (Yoo et al., 2014). Subsequent hematomas in the fourth ventricle and on the cerebellar surface caused decreased granule cell density, decreased cerebellar volume and resulted abnormal open field testing behavior, and motor impairment on Rotarod testing in older mice (Yoo et al., 2014), which is exacerbated by inflammation (Tremblay et al., 2017). The effects of isolated posterior fossa blood exposure in the absence of intraventricular hemorrhage on cerebellar development have never been directly tested *in vivo*.

In this study, we developed a novel model of isolated posterior fossa subarachnoid hemorrhage in neonatal mice to directly examine the effects of blood exposure on cerebellar development. Our model avoids direct injury to the cerebellar parenchyma and isolates injury related to blood components. We examined acute and long-term effects on cerebellar biology, anatomy, and animal behavior following CHI. We hypothesized that exposure of the developing cerebellum to blood would result in disruption to multiple developmental programs leading to long-term cellular/anatomic abnormalities and motor deficits. Secondarily, we hypothesized that neuroinflammation may strongly contribute to the underlying injury mechanism and that treatment with an anti-inflammatory may be neuroprotective.

Materials and methods

Animals

This study was carried out in accordance with the recommendations in the Guide for the Care and Use of Laboratory Animals of the National Institutes of Health and was approved by the Institutional Animal Care and Use Committee (IACUC) at University of Washington (Protocol Number: IACUC00006). Mice from the CD1 strain were bred and housed in Optimice cages with aspen bedding at the Seattle Children's Research Institute specific pathogen-free (SPF) vivarium facility on a 14/10 hour light/dark cycle. All mice were monitored closely by both laboratory and veterinary staff. The day of birth was designated as postnatal day 0 (P0).

Posterior fossa injection procedure

On P6, mice underwent posterior fossa injections under anesthesia with isoflurane. Peak EGL proliferation occurs at P6. We chose this to model the timing of injury in ELGANs which also correlates with peak EGL proliferation. A single 8–10 mm vertical incision was made overlying the posterior calvaria (Figure 1A). Trunk blood from an adult CD1 mouse was obtained and anticoagulated with heparin at a ratio of 100 μl heparin to 900 μl of blood. For the CHI group, 20 μl of trunk blood was injected into the posterior fossa with a 28-gauge insulin needle at the midline position, 2.5 mm rostral from Lambda under direct visualization. Control group animals underwent posterior fossa injection with

20 μl of heparin containing artificial cerebrospinal fluid (aCSF) (Wei and Ramirez, 2019) as outlined above. Following injection, the needle was gently removed, and the skull defect was covered with Vetbond™ tissue adhesive (3M). Skin closure was performed with 7.0 Ethilon® nylon suture (Ethicon). Animals received either buprenorphine (opioid: 2 μg/g of body weight) or ketoprofen (non-steroidal anti-inflammatory: 5 μg/g of body weight) for analgesia, to assess the role of inflammation in injury. Mice were warmed and monitored closely during the entire procedure and recovered under a heat lamp until they were noted to have consistent spontaneous movements prior to return to their home cages.

Sample preparation

On P8 or P42, mice were pulsed with 5-bromo-2'-deoxyuridine (BrdU) *via* intraperitoneal injections (10 μg/g of body weight) 2 h prior to sacrifice. P8 was chosen to assess the immediate impact of injury, while P42 was chosen to assess the outcome, when cerebellar maturation is complete. On P8, mice were sacrificed *via* rapid decapitation, tissue was harvested and then fixed in 4% paraformaldehyde (PFA) overnight. On P42, mice underwent both cardiac fixation with 4% PFA infusion and drop fixation in 4% PFA overnight. At both timepoints, tissue was then equilibrated in 30% sucrose made in phosphate-buffered saline (PBS). Cerebellar tissue was isolated, placed in Tissue-Tek® O.C.T compound and stored at−80°C. Sections were performed at 18–20 μm on a freezing microtome.

Immunohistochemistry

Sections were dried at room temperature for 60 min, baked at 45°C for 30 min, and washed in PBS. Sections undergoing BrdU staining for were bathed in 2N HCl for 30 min. All sections underwent antigen retrieval by boiling sections in 10 mM sodium citrate for 10–15 min. Sections were then washed three times with PBS with 0.125% Triton X-100 (PBX) and blocked in 5% donkey serum in PBX in a humidified chamber for 90 min at room temperature. Sections were incubated at 4°C with primary antibodies in a humidified chamber overnight. The following day, sections were washed in PBX and then incubated with species-specific secondary antibodies conjugated with Alexa 488, 568 or 594 fluorophores (Invitrogen) for 90 min at room temperature. Sections were counterstained with DAPI (4',6-Diamidino-2-Phenylindole, Dihydrochloride; Invitrogen; D1306) and cover-slipped with Fluoromount-G (Southern Biotech, Cat. No. 0100-01). Primary antibodies used included: rat anti-BrdU (1:100, Abcam), mouse anti-Calbindin (1:20, Abcam), rabbit anti-GFAP (1:1,500, Dako), rabbit anti-Ki67 (1:150, Novus), mouse anti-Parvalbumin (1:5,000, Swant), rabbit anti-BLBP (1:400, Abcam).

Rotarod assay

At P35, all mice underwent motor learning and coordination testing using the Rota-Rod 2 (Med Associates Inc.). On day 1 of testing, each mouse underwent three trials, and on days 2 and 3, each mouse underwent two trials. Each trial consisted of programmed acceleration from 4 to 40 RPM over a period of 3 min and were separated by 120 min. The time spent on the rotarod was recorded for each trial. Statistical significance was defined as $p < 0.05$ by two-way ANOVA with Tukey's post-test and performed in GraphPad Prism v8.4.1(460) (GraphPad Software LLC., San Diego, USA).

Inverted screen test assay

At P38, all mice underwent strength and coordination testing using the inverted screen test (Kondziella, 1964). Mice were placed in the center of a wire mesh, which was then rotated into the inverted position (mouse headfirst) and held approximately 30 cm above a padded surface for a maximum of 120 s. The time spent in the inverted position was recorded for each mouse. Statistical significance was defined as $p < 0.05$ by one-way ANOVA with Tukey's post-test and performed in GraphPad Prism v8.4.1(460) (GraphPad Software LLC., San Diego, USA).

Quantitative analysis

All image and quantitative analysis were performed with Olympus VS-Desktop software and ImageJ 1.52p (NIH, Bethesda, Maryland, USA) software. Sections underwent extended focal imaging (EFI) at 10X and 20X with the Olympus VS-120 slide-scanner microscope and confocal imaging at 20X and 40X. To evaluate the local effect of hemorrhage at P8, areas of red blood cell (RBC) aggregation were identified, and neighboring lobules were selected for analysis. Quantitative data was collected from comparable sections from each treatment group. At P8, measurements of EGL thickness ($n = 2$ sections/animal, 4 animals/treatment group), Calbindin$^+$ PC density ($n = 4$ sections/animal, three animals/treatment group), GFAP$^+$ Bergmann glial (BG) fiber crossings ($n = 3$ sections/animal, three animals/treatment group), and BrDU/Ki67$^+$ labeling index (BrDU/Ki67$^+$ cells/DAPI$^+$ cells) were obtained ($n = 3$ sections/animal, three animals/treatment group). At P42, measurements of PC density, BG fiber crossings, and Parvalbumin$^+$ molecular layer interneuron (MLI) density ($n = 3$ sections/animal, three animals/treatment group) were obtained from lobules VI-X. Statistical significance was defined as $p < 0.05$ by one-way ANOVA with Tukey's post-test and performed in GraphPad Prism v8.4.1(460) (GraphPad Software LLC., San Diego, USA).

Results

Blood exposure at P6, during peak EGL proliferation, caused significant abnormalities in adjacent regions by P8

As shown in Figure 1B, regions of blood exposure were readily identified and we limited our analyses to these regions

10.3389/fnmol.2023.1161086

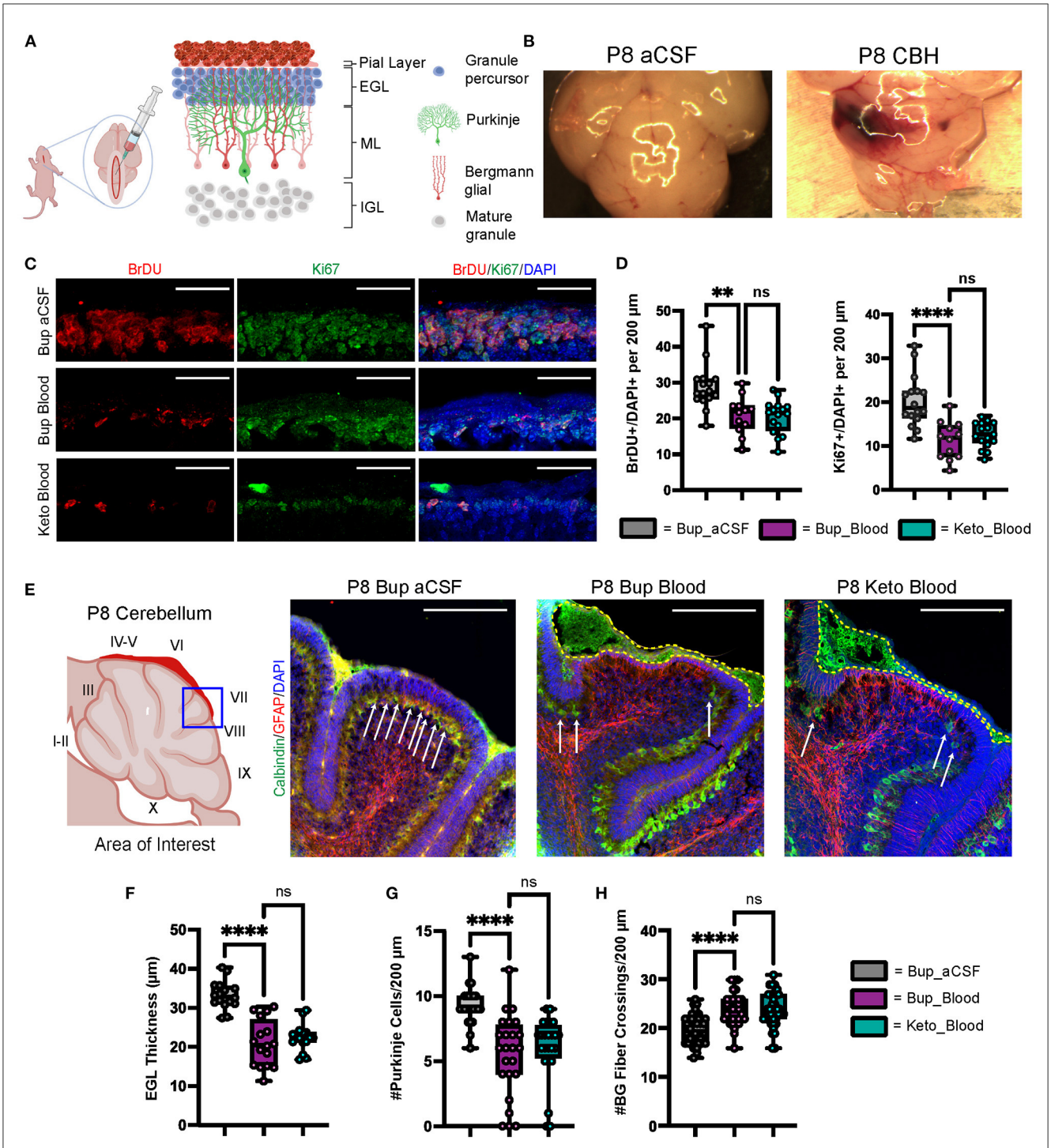

FIGURE 1
CHI results in decreased BrDU and Ki67 labeling indices, thinning of the EGL, decreased PC density, and increased BG fiber crossings at P8. **(A)** Schematic illustrating isolated posterior fossa hemorrhage model with typical P6 cerebellar architecture. **(B)** Representative comparative images of gross findings between aCSF and CHI groups; note large hematoma formation overlying left cerebellar hemisphere in the CHI specimen. **(C)** Representative confocal images at 40X of BrDU and Ki67 staining within the EGL. Only cells within the EGL were included in analysis. Scale bars are 25 µm. **(D)** Quantification of labeling indices for BrDU (left) and Ki67 (right); data obtained from 200 µm segment from lobule VI and VII ($N = 2$, $n = 12$ for Bup_Blood; $N = 3$, $n = 16$ for Bup_aCSF and Keto_Blood). **(E)** Representative confocal images at 20X magnification of lobule VII demonstrating differences in local findings including presence of large RBC collections (yellow dashed outline), PC density (white arrows), thickness of EGL, and architecture of BG fibers. Scale bars are 100 µm. **(F)** Quantification of EGL thickness for all treatment groups ($N = 4$, $n = 16$). **(G)** Quantification of PC density in lobule VI and VII for all treatment groups ($N = 3$, $n = 24$). **(H)** Quantification of BG fiber crossings in lobule I, VII-IX for all treatment groups ($N = 3$, $n = 27$). Significance defined as $p < 0.05$ by one-way ANOVA with Tukey post-test. Data are presented as SEM with minimum and maximum values. N = number of animals per group included for analysis; n = number of section segments per group included for analysis. **p-value ≤ 0.01; ****p-value ≤ 0.0001.

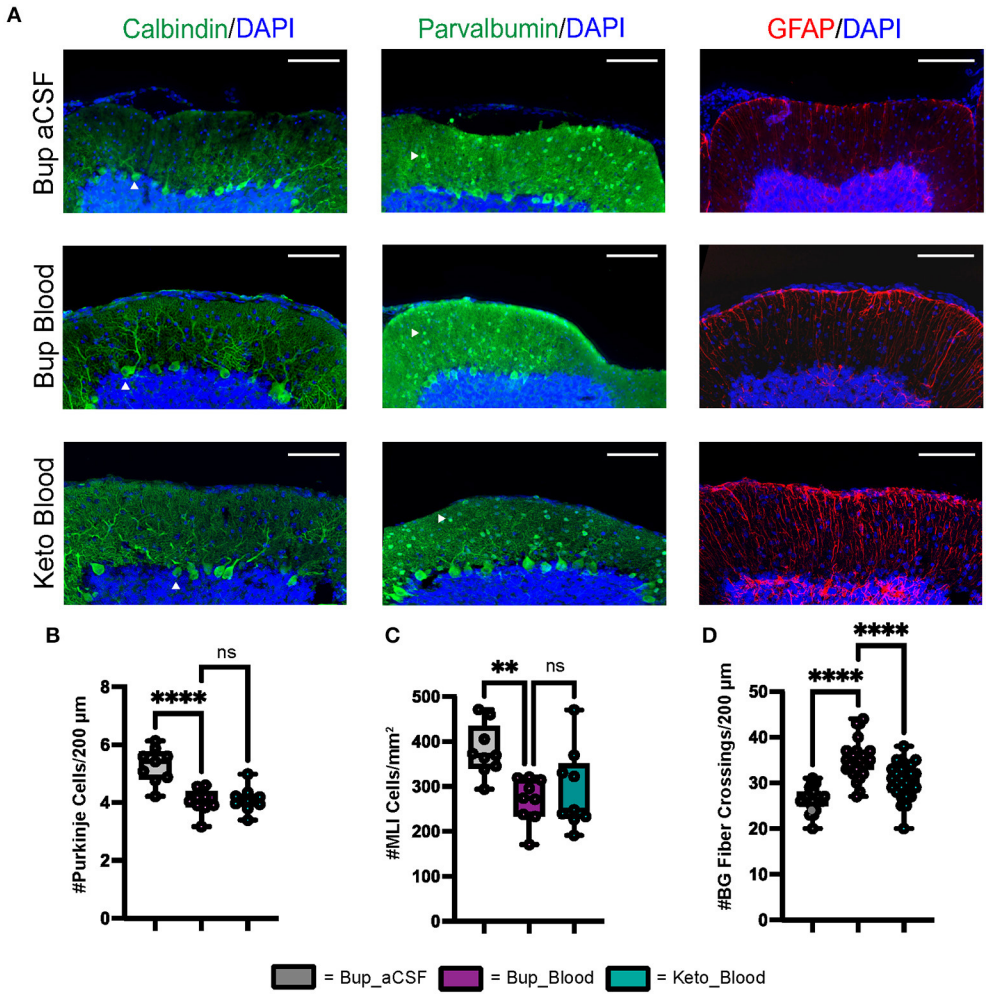

FIGURE 2
CHI results in decreased PC density, decreased MLI density, and increased BG fiber crossings within the ML at P42. **(A)** Representative confocal images at 20X demonstrating difference in PC (white arrowhead) density (left), MLI (white arrowhead) density (middle), and BG fiber density and morphology (right). Scale bars are 100 μm. **(B)** Quantification of PC density in lobule VI-X for all treatment groups ($N = 3$, $n = 9$). **(C)** Quantification of MLI density in lobule VI-X for all treatment groups ($N = 3$, $n = 9$). **(D)** Quantification of BG fiber crossings within the ML for all treatment groups ($N = 3$, $n = 27$). Significance defined as $p < 0.05$ by one-way ANOVA with Tukey's post-test. Data are presented as SEM with minimum and maximum values. N = number of animals per group included for analysis, n = number of section segments per group included for analysis.

in vermis and paravermis cerebellar lobules V-VII. Compared with aCSF at P8, blood exposure resulted in a significantly decreased EGL proliferation as measured by BrdU and Ki67 labeling ($p = 0.0015$ and $p < 0.0001$, respectively) (Figures 1C, D). Blood exposure also significantly decreased EGL thickness compared to aCSF ($p < 0.0001$) (Figures 1C, E, F). We also saw significant loss of (Calbindin +) Purkinje cells in regions of blood exposure (Figures 1E, G). GFAP+ Bergman glial fiber crossings were significantly increased following blood exposure compared to aCSF-buprenorphine ($p < 0.0001$) (Figures 1E, H) with erratic Bergman glial fiber branching and altered fiber architecture, compared to the typical ordered fiber structure seen in the aCSF groups. Additionally, breaks in Bergman glial fibers and endplate detachment were noted (Figure 1E and not shown). There were no differences between blood exposed animals that received buprenorphine vs. ketoprofen for BrdU labeling, Ki67 labeling, EGL thickness, Purkinje cell density, and Bergman glial crossings ($p = 0.9729$, $p = 0.7645$, $p = 0.63$, $p = 0.6873$, and $p = 0.9531$, respectively).

Regional morphological changes were persistant at P42, in the mature cerebellum

Similar to findings at P8, blood exposure was associated with decreased Purkinje cell density at P42 ($p < 0.0001$) (Figures 2A, B). Blood exposure was also associated with decreased MLI density compared to aCSF ($p = 0.0058$) (Figures 2A, C). There was no significant difference between blood exposed animals that received ketoprofen vs. buprenorphine for PC density and MLI density ($p = 0.9665$ and $p = 0.7783$, respectively) (Figures 2A–C).

Similar to findings at P8, blood exposure was associated with abnormal Bergman glial fiber branching and increased fiber crossings in animals that received buprenorphine at P42

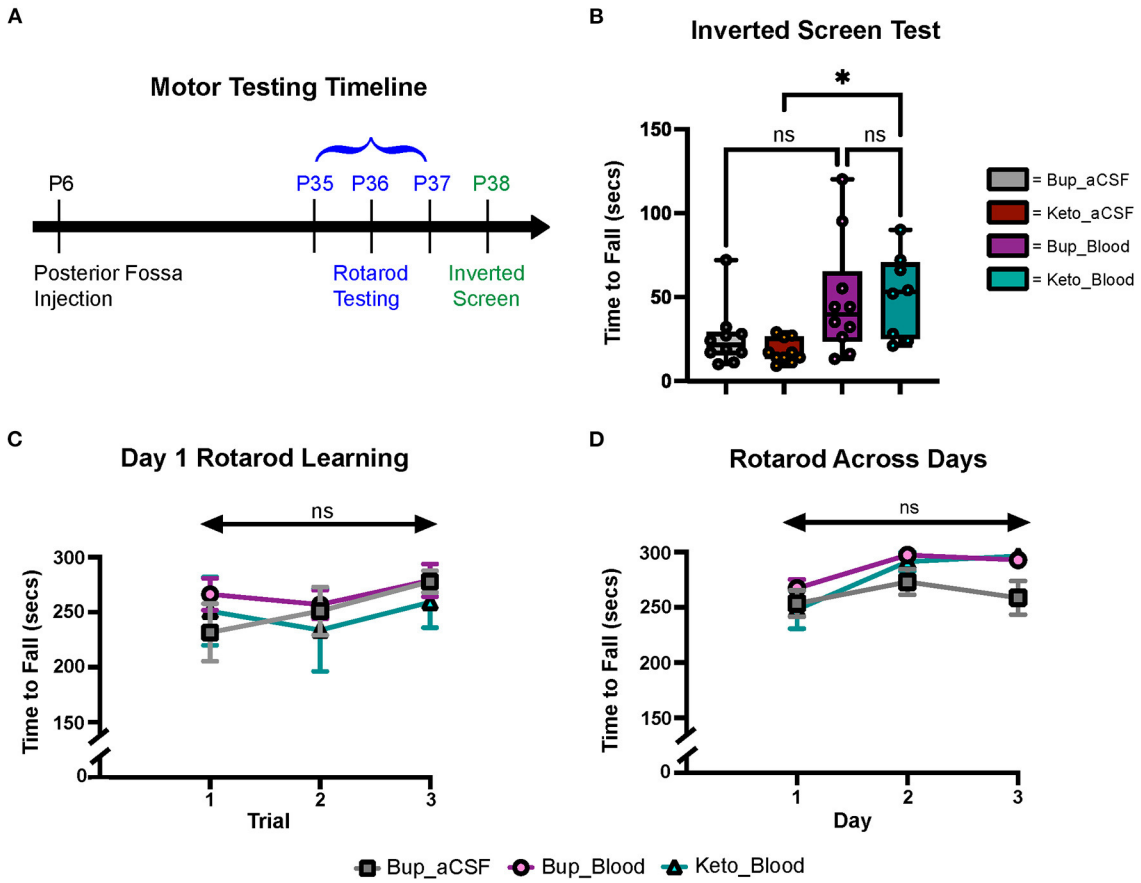

FIGURE 3
CHI did not result in significant motor learning/coordination deficits. **(A)** Schematic of motor testing assays and timeline. **(B)** Quantification of time to fall for the inverted screen test for all groups ($N = 10$*)†. **(C)** Quantification of the time to fall for Day 1 of Rotarod training for all groups ($N = 10$*)‡. **(D)** Quantification of the time to fall for Days 1-3 of Rotarod training for all groups ($N = 10$*)‡. Data are presented as mean ± SEM **(B)** or SEM with minimum and maximum values **(C, D)**. N = number of animals per group included for analysis. *Keto_Blood group with $N = 8$. †Significance defined as $p < 0.05$ by one-way ANOVA with Tukey's post-test. ‡Significance defined as $p < 0.05$ by two-way ANOVA with Tukey's post-test.

($p < 0.0001$) (Figures 2A, D). Blood exposed animals that received ketoprofen had significantly fewer Bergman glial fiber crossings compared to those receiving buprenorphine ($p < 0.0001$) (Figure 2D). Blood exposure did not result in significant difference in Bergman glial soma density, either in typical position or ectopic position within the molecular layer (Supplementary Figure 1).

Neonatal blood exposure did not result in significant gross motor learning/coordination deficits in older animals

Gross motor learning and coordination were assessed in mature animals at P35–38 (Figure 3A). Results from the inverted screen test demonstrated no significant differences between the blood and aCSF animals receiving buprenorphine ($p = 0.1580$); however, animals in the blood-ketoprofen group were noted to remain suspended for significantly longer than animals in the aCSF-ketoprofen group ($p = 0.024$) (Figure 3B). There were no significant differences noted between groups on Rotarod testing (Figures 3C, D).

Discussion

To examine how preterm and neonatal cerebellar bleeds during maximal EGL proliferation in humans alters cerebellar development, we developed a novel murine model of isolated posterior fossa subarachnoid hemorrhage at P6, when maximal EGL proliferation occurs in mice. Subarachnoid blood exposure resulted in immediate and sustained morphological abnormalities to multiple cell populations immediately adjacent to the blood, especially granule and Purkinje cells, BG, and MLIs.

Multiple studies have demonstrated that PCs are exquisitely sensitive to injury, with hypoxic and ischemic insults resulting in damage to PCs in both animal models and human studies (Barenberg et al., 2001; Hausmann et al., 2007; Kántor et al., 2007; Bartschat et al., 2012; Sathyanesan et al., 2018). Importantly, PCs are essential to the normal development of the cerebellum, as PC-derived Sonic hedgehog (Shh) protein is a key driver of granule cell precursor proliferation within the overlying EGL (Smeyne et al., 1995; Dahmane and Ruiz i Altaba, 1999; Wechsler-Reya and Scott, 1999; Lewis et al., 2004; Fleming and Chiang, 2015; De Luca et al., 2016). In the present study, subarachnoid hemorrhage was modeled

at P6, a key time point in cerebellar development characterized by rapid expansion of granule neuron progenitorss in the EGL and active Shh expression by PCs. Following CHI, we found localized thinning of the EGL and decreased EGL BrDU/Ki67 labeling at P8 (Figure 1). No changes to TUNEL/Caspase 3 staining were evident at P8 (data not shown) and we did not conduct immediate pulse chase experiments to determine if early differentiation contributed to this phenotype. However, it is likely that EGL thinning was result of a combination of immediate cell death, increased differentiation, and proliferative loss of EGL progenitors at these early timepoints immediately after injury. We also saw immediate localized loss of PCs, with significant decreased density at P8 that was sustained at P42 (Figures 1, 2). This result is in contrast to Yoo et al. (2014), who reported no significant change in PC count in adult mice after induction of neonatal cerebellar hemorrhage with a bacterial collagenase injection model. One caveat to our study is that we injected adult vs. age matched blood. We cannot distinguish if loss is due to a direct effect on each population independently, however, loss of PC derived Shh mitotic most certainly contributed to diminished granule cell precursor proliferation.

Recently, Bayin et al. (2018) demonstrated that the developing mouse cerebellum has intrinsic capacity for PC regeneration/replenishment by immature PC precursors. The regeneration capacity of these cells decreases during the first postnatal week at ∼P5 (Bayin et al., 2018). In this study, blood exposure at P6 resulted in persistent decreases in PC density at P42, demonstrating significant long-term effect of CHI occurring at this developmental timepoint on the PC population (Figure 2B). This is important, as PC loss has been associated with multiple neurodevelopmental disorders in children, including autism spectrum disorder (ASD), many of which are present in ELGANs post cerebellar hemorrhage (Fatemi et al., 2002; Jeong et al., 2014; Skefos et al., 2014). Additionally, this finding is supportive of the limited replenishment capacity of the mouse cerebellum after the first postnatal week.

In addition to significant PC loss, our results demonstrate CHI has long-term effects on MLIs, with significantly decreased MLI density noted at P42 (Figure 2C). Interneuron precursor cells undergo significant proliferation and migration during development of the cerebellum, a process which is supported by PC (Fahrion et al., 2013; Galas et al., 2017). Specifically, PC-derived Shh has been demonstrated to regulate neural stem-cell like primary progenitors within the WM which give rise to inhibitory interneurons (Fleming et al., 2013). Later in development, two subtypes (Stellate cells and Basket cells) will migrate into the cortex, a process which is active in mice until P16 and may be disrupted by early postnatal insults (Zhang and Goldman, 1996). Recently, data from Sergaki et al. (2017) demonstrated that neurotrophic factors expressed by PCs help regulate MLI survival, suggesting that damage to PCs in the postnatal cerebellum may also result in decreased MLI survival. We postulate that CHI induced PC loss may result in impaired interactions between PCs and MLIs, resulting in diminished development of the MLI population.

BG are specialized unipolar astrocytes which have been found to guide GC precursor migration from the EGL to the IGL and may contribute to PC dendrite maturation (Rakic, 1971; Yamada et al., 2000; Lippman et al., 2008; Cheng et al., 2018). We found that CHI was associated with increased BG fiber crossings and abnormal fiber architecture at both P8 and P42 (Figures 1E, H, D), but no difference in BG soma density (Supplementary Figure 1A). These data suggest that CHI primarily affects the branching of BG fibers rather than proliferation or maintenance of the BG population. The increase in fiber crossings likely represents reactive gliosis in response to CHI, as immature BG have previously been shown to be capable of increasing GFAP expression in response to injury (Lafarga et al., 1998).

Despite effects on multiple cell types within the developing cerebellum, we did not see statistically significant motor deficits on Rotarod or inverted screen test assays following CHI (Figures 3B–D). Subjectively, mice in the CHI treatment groups were noted to spend more time clinging to the rotating rod and less time demonstrating coordinated walking during the Rotarod trials compared to the aCSF mice. Additionally, mice in the aCSF groups exhibited increased exploratory behavior during the inverted screen test, while CHI mice tended to remain in a small area with less movement. It is possible that this increase in exploratory behavior resulted in increased likelihood of grip loss and falling from the wire mesh, explaining why mice in the Keto-aCSF group fell off of the mesh more quickly than mice in the Keto-CHI group (Figure 3B). Moreover, it is possible that subtle motor deficits may have been found utilizing different behavior assays, such as eyeblink conditioning or vestibulo-ocular reflex analysis. This is a limitation of our current study and requires further investigation to understand the relationship between CHI and motor deficits. There is ample evidence from human cerebellar bleed patients that severity of functional deficits is dependent on injury size and topography (Brossard-Racine and Limperopoulos, 2021).

Secondarily, we compared the use of the opiate buprenorphine and the non-steroidal anti-inflammatory drug (NSAID) ketoprofen in order to investigate the possible role of neuroinflammation in injury. The use of ketoprofen in our model was associated with variable results, but did not demonstrate a significant neuroprotective effect. In the acute injury phase (P6-8), we found no significant difference post CHI in EGL thickness, PC density, BrDU/Ki67 labeling indices, and BG crossings (Figure 1) between buprenorphine and ketoprofen cohorts. Similarly, we saw no significant difference in PC density, MLI density, oligodendrocyte density, or BG soma density at P42 (Figure 2; Supplementary Figure 1). We did see a significant decrease in BG fiber crossings at P42 in CHI mice treated with ketoprofen compared to those treated with buprenorphine (Figure 2D). Taken together, these data suggest that anti-inflammatory treatment does not have a profound protective effect on cerebellar development in our model of CHI; however, additional studies are required to further elucidate the role of neuroinflammation, particularly with regards to reactive Bergmann gliosis.

In summary, we developed a novel neonatal mouse model of isolated posterior fossa SAH to model neonatal CHI, directly examining the effects of blood exposure on cerebellar development.

Our data demonstrates that exposure of the developing cerebellum to blood results in immediate disruptions to multiple aspects of cellular development and most strongly suggests the involvement of PC loss in the pathophysiology.

Data availability statement

The raw data supporting the conclusions of this article will be made available by the authors, without undue reservation.

Ethics statement

The animal study was reviewed and approved by Institutional Animal Care and Use Committee University of Washington.

Author contributions

This study was conceived by KM, DB, JS, and CT. All experiments were designed and performed by DB, CT, and JS. KM and DB wrote the manuscript with input from all authors. All authors contributed to the article and approved the submitted version.

Funding

This work was funded by NIH R37NS095733 to KM.

Conflict of interest

The authors declare that the research was conducted in the absence of any commercial or financial relationships that could be construed as a potential conflict of interest.

Publisher's note

All claims expressed in this article are solely those of the authors and do not necessarily represent those of their affiliated organizations, or those of the publisher, the editors and the reviewers. Any product that may be evaluated in this article, or claim that may be made by its manufacturer, is not guaranteed or endorsed by the publisher.

Supplementary material

The Supplementary Material for this article can be found online at: https://www.frontiersin.org/articles/10.3389/fnmol.2023.1161086/full#supplementary-material

SUPPLEMENTARY FIGURE 1
CHI did not result in significant differences in BG soma density or ectopic positioning of BG soma at P42. **(A)** Quantification of BG soma density for all treatment groups ($N = 1$, $n = 9$). **(B)** Quantification of BG soma density noted in ectopic positioning for all treatment groups ($N = 1$, $n = 9$). Significance defined as $p < 0.05$ by one-way ANOVA with Tukey's post-test. Data are presented as SEM with minimum and maximum values. N = number of animals per group included for analysis, n = number of sections per group included for analysis.

References

Abraham, H., Tornoczky, T., Kosztolanyi, G., and Seress, L. (2001). Cell formation in the cortical layers of the developing human cerebellum. *Int. J. Dev. Neurosci.* 19, 53–62. doi: 10.1016/S0736-5748(00)00065-4

Aldinger, K. A., Timms, A. E., Thomson, Z., Mirzaa, G. M., Bennett, J. T., Rosenberg, A. B., et al. (2019). Redefining the etiologic landscape of cerebellar malformations. *Am. J. Hum. Genet.* 105, 606–615. doi: 10.1016/j.ajhg.2019.07.019

Barenberg, P., Strahlendorf, H., and Strahlendorf, J. (2001). Hypoxia induces an excitotoxic-type of dark cell degeneration in cerebellar Purkinje neurons. *Neurosci. Res.* 40, 245–254. doi: 10.1016/S0168-0102(01)00234-6

Barron, T., and Kim, J. H. (2020). Preterm birth impedes structural and functional development of cerebellar purkinje cells in the developing baboon cerebellum. *Brain Sci.* 10:897. doi: 10.3390/brainsci10120897

Bartschat, S., Fieguth, A., Könemann, J., Schmidt, A., and Bode-Jänisch, S. (2012). Indicators for acute hypoxia–an immunohistochemical investigation in cerebellar Purkinje-cells. *Forensic Sci. Int.* 223, 165–170. doi: 10.1016/j.forsciint.2012.08.023

Bayin, N. S., Wojcinski, A., Mourton, A., Saito, H., Suzuki, N., and Joyner, A. L. (2018). Age-dependent dormant resident progenitors are stimulated by injury to regenerate Purkinje neurons. *Elife* 7. doi: 10.7554/eLife.39879.034

Boswinkel, V., Steggerda, S. J., Fumagalli, M., Parodi, A., Ramenghi, L. A., Groenendaal, F., et al. (2019). The CHOPIn study: a multicenter study on cerebellar hemorrhage and outcome in preterm infants. *Cerebellum* 18, 989–998. doi: 10.1007/s12311-019-01053-1

Brossard-Racine, M., and Limperopoulos, C. (2021). Cerebellar injury in premature neonates: Imaging findings and relationship with outcome. *Semin. Perinatol.* 45, 151470. doi: 10.1016/j.semperi.2021.151470

Buddington, R. K., Chizhikov, V. V., Iskusnykh, I. Y., Sable, H. J., Sable, J. J., Holloway, Z. R., et al. (2018). A phosphatidylserine source of docosahexanoic acid improves neurodevelopment and survival of preterm pigs. *Nutrients* 10:637. doi: 10.3390/nu10050637

Cheng, F. Y., Fleming, J. T., and Chiang, C. (2018). Bergmann glial Sonic hedgehog signaling activity is required for proper cerebellar cortical expansion and architecture. *Dev. Biol.* 440, 152–166. doi: 10.1016/j.ydbio.2018.05.015

Chizhikov, D., Buddington, R. K., and Iskusnykh, I. Y. (2020). Effects of phosphatidylserine source of docosahexaenoic acid on cerebellar development in preterm pigs. *Brain Sci.* 10:475. doi: 10.3390/brainsci10080475

Consalez, G. G., Goldowitz, D., Casoni, F., and Hawkes, R. (2020). Origins, development, and compartmentation of the granule cells of the cerebellum. *Front. Neural Circuits* 14:611841. doi: 10.3389/fncir.2020.611841

Dahmane, N., and Ruiz i Altaba, A. (1999). Sonic hedgehog regulates the growth and patterning of the cerebellum. *Development* 126, 3089–3100. doi: 10.1242/dev.126.14.3089

De Luca, A., Cerrato, V., Fuc,à, E., Parmigiani, E., Buffo, A., and Leto, K. (2016). Sonic hedgehog patterning during cerebellar development. *Cell. Mol. Life Sci.* 73, 291–303. doi: 10.1007/s00018-015-2065-1

Dijkshoorn, A. B. C., Turk, E., Hortensius, L. M., van der Aa, N. E., Hoebeek, F. E., Groenendaal, F., et al. (2020). Preterm infants with isolated cerebellar hemorrhage show bilateral cortical alterations at term equivalent age. *Sci. Rep.* 10, 5283. doi: 10.1038/s41598-020-62078-9

D'Mello, A. M., and Stoodley, C. J. (2015). Cerebro-cerebellar circuits in autism spectrum disorder. *Front. Neurosci.* 9, 408. doi: 10.3389/fnins.2015.00408

Fahrion, J., Komuro, Y., Ohno, N., Littner, Y., Nelson, C., Kumada, T., et al. (2013). Cerebellar patterning. *Comprehensive Developmental Neuroscience: Patterning and Cell Type Specification in the Developing CNS and PNS*, 211–225. doi: 10.1016/B978-0-12-397265-1.00042-3

Fatemi, S. H., Halt, A. R., Realmuto, G., Earle, J., Kist, D. A., Thuras, P., et al. (2002). Purkinje cell size is reduced in cerebellum of patients with autism. *Cell. Mol. Neurobiol.* 22, 171–175. doi: 10.1023/A:1019861721160

Fleming, J., and Chiang, C. (2015). The Purkinje neuron: A central orchestrator of cerebellar neurogenesis. *Neurogenesis* 2:e1025940. doi: 10.1080/23262133.2015.1025940

Fleming, J. T., He, W., Hao, C., Ketova, T., Pan, F. C., Wright, C. C., et al. (2013). The Purkinje neuron acts as a central regulator of spatially and functionally distinct cerebellar precursors. *Dev. Cell* 27, 278–292. doi: 10.1016/j.devcel.2013.10.008

Galas, L., Bénard, M., Lebon, A., Komuro, Y., Schapman, D., Vaudry, H., et al. (2017). Postnatal migration of cerebellar interneurons. *Brain Sci.* 7:62. doi: 10.3390/brainsci7060062

Gano, D., and Barkovich, A. J. (2019). Cerebellar hypoplasia of prematurity: causes and consequences. *Handb. Clin. Neurol.* 162, 201–216. doi: 10.1016/B978-0-444-64029-1.00009-6

Haines, K. M., Wang, W., and Pierson, C. R. (2013). Cerebellar hemorrhagic injury in premature infants occurs during a vulnerable developmental period and is associated with wider neuropathology. *Acta. Neuropathol. Commun.* 1, 69. doi: 10.1186/2051-5960-1-69

Haldipur, P., Bharti, U., Alberti, C., Sarkar, C., Gulati, G., Iyengar, S., et al. (2011). Preterm delivery disrupts the developmental program of the cerebellum. *PLoS ONE* 6:e23449. doi: 10.1371/journal.pone.0023449

Hausmann, R., Seidl, S., and Betz, P. (2007). Hypoxic changes in Purkinje cells of the human cerebellum. *Int. J. Legal Med.* 121, 175–183. doi: 10.1007/s00414-006-0122-x

Iskusnykh, I. Y., Buddington, R. K., and Chizhikov, V. V. (2018). Preterm birth disrupts cerebellar development by affecting granule cell proliferation program and Bergmann glia. *Exp. Neurol.* 306, 209–221. doi: 10.1016/j.expneurol.2018.05.015

Iskusnykh, I. Y., and Chizhikov, V. V. (2022). Cerebellar development after preterm birth. *Front. Cell Dev. Biol.* 10:1068288. doi: 10.3389/fcell.2022.1068288

Iskusnykh, I. Y., Fattakhov, N., Buddington, R. K., and Chizhikov, V. V. (2021). Intrauterine growth restriction compromises cerebellar development by affecting radial migration of granule cells via the JamC/Pard3a molecular pathway. *Exp. Neurol.* 336, 113537. doi: 10.1016/j.expneurol.2020.113537

Jeong, J. W., Tiwari, V. N., Behen, M. E., Chugani, H. T., and Chugani, D. C. (2014). In vivo detection of reduced Purkinje cell fibers with diffusion MRI tractography in children with autistic spectrum disorders. *Front. Hum. Neurosci.* 8, 110. doi: 10.3389/fnhum.2014.00110

Johnsen, S. D., Bodensteiner, J. B., and Lotze, T. E. (2005). Frequency and nature of cerebellar injury in the extremely premature survivor with cerebral palsy. *J. Child Neurol.* 20, 60–64. doi: 10.1177/08830738050200011001

Kántor, O., Schmitz, C., Feiser, J., Brasnjevic, I., Korr, H., Busto, R., et al. (2007). Moderate loss of cerebellar Purkinje cells after chronic bilateral common carotid artery occlusion in rats. *Acta Neuropathol.* 113, 549–558. doi: 10.1007/s00401-007-0204-y

Kondziella, W. (1964). [A new method for the measurement of muscle relaxation in white mice]. *Arch. Int. Pharmacodyn. Ther.* 152, 277–284.

Lafarga, M., Andres, M. A., Calle, E., and Berciano, M. T. (1998). Reactive gliosis of immature Bergmann glia and microglial cell activation in response to cell death of granule cell precursors induced by methylazoxymethanol treatment in developing rat cerebellum. *Anat. Embryol.* 198, 111–122. doi: 10.1007/s004290050169

Lewis, P. M., Gritli-Linde, A., Smeyne, R., Kottmann, A., and McMahon, A. P. (2004). Sonic hedgehog signaling is required for expansion of granule neuron precursors and patterning of the mouse cerebellum. *Dev. Biol.* 270, 393–410. doi: 10.1016/j.ydbio.2004.03.007

Limperopoulos, C., Bassan, H., Gauvreau, K., Robertson, R. L. Jr., Sullivan, N. R., Benson, C. B., et al. (2007). Does cerebellar injury in premature infants contribute to the high prevalence of long-term cognitive, learning, and behavioral disability in survivors? *Pediatrics* 120, 584–593. doi: 10.1542/peds.2007-1041

Limperopoulos, C., Chilingaryan, G., Guizard, N., Robertson, R. L., and Du Plessis, A. J. (2010). Cerebellar injury in the premature infant is associated with impaired growth of specific cerebral regions. *Pediatr. Res.* 68, 145–150. doi: 10.1203/PDR.0b013e3181e1d032

Limperopoulos, C., Chilingaryan, G., Sullivan, N., Guizard, N., Robertson, R. L., and du Plessis, A. J. (2014). Injury to the premature cerebellum: outcome is related to remote cortical development. *Cereb. Cortex* 24, 728–736. doi: 10.1093/cercor/bhs354

Lippman, J. J., Lordkipanidze, T., Buell, M. E., Yoon, S. O., and Dunaevsky, A. (2008). Morphogenesis and regulation of Bergmann glial processes during Purkinje cell dendritic spine ensheathment and synaptogenesis. *Glia* 56, 1463–1477. doi: 10.1002/glia.20712

Matsufuji, M., Sano, N., Tsuru, H., and Takashima, S. (2017). Neuroimaging and neuropathological characteristics of cerebellar injury in extremely low birth weight infants. *Brain Dev.* 39, 735–742. doi: 10.1016/j.braindev.2017.04.011

Nosarti, C., Giouroukou, E., Micali, N., Rifkin, L., Morris, R. G., and Murray, R. M. (2007). Impaired executive functioning in young adults born very preterm. *J. Int. Neuropsychol. Soc.* 13, 571–581. doi: 10.1017/S1355617707070725

Poretti, A., Leventer, R. J., Cowan, F. M., Rutherford, M. A., Steinlin, M., Klein, A., et al. (2008). Cerebellar cleft: a form of prenatal cerebellar disruption. *Neuropediatrics* 39, 106–112. doi: 10.1055/s-2008-1081460

Rakic, P. (1971). Neuron-glia relationship during granule cell migration in developing cerebellar cortex. a golgi and electronmicroscopic study in macacus rhesus. *J. Comp. Neurol.* 141, 283–312. doi: 10.1002/cne.901410303

Sathyanesan, A., Kundu, S., Abbah, J., and Gallo, V. (2018). Neonatal brain injury causes cerebellar learning deficits and Purkinje cell dysfunction. *Nat. Commun.* 9, 3235. doi: 10.1038/s41467-018-05656-w

Scelsa, B., Cutillo, G., Lanna, M. M., Righini, A., Balestriero, M. A., Brazzoduro, V., et al. (2022). Prenatal diagnosis and neurodevelopmental outcome in isolated cerebellar hypoplasia of suspected hemorrhagic etiology: a retrospective cohort study. *Cerebellum* 21, 944–953. doi: 10.1007/s12311-021-01341-9

Sergaki, M. C., López-Ramos, J. C., Stagkourakis, S., Gruart, A., Broberger, C., Delgado-García, J. M., et al. (2017). Compromised survival of cerebellar molecular layer interneurons lacking gdnf receptors GFRα1 or RET impairs normal cerebellar motor learning. *Cell Rep.* 19, 1977–1986. doi: 10.1016/j.celrep.2017.05.030

Skefos, J., Cummings, C., Enzer, K., Holiday, J., Weed, K., Levy, E., et al. (2014). Regional alterations in purkinje cell density in patients with autism. *PLoS ONE* 9:e81255. doi: 10.1371/journal.pone.0081255

Smeyne, R. J., Chu, T., Lewin, A., Bian, F., Sanlioglu, S., Kunsch, C., et al. (1995). Local control of granule cell generation by cerebellar Purkinje cells. *Mol. Cell. Neurosci.* 6, 230–251. doi: 10.1006/mcne.1995.1019

Spoto, G., Amore, G., Vetri, L., Quatrosi, G., Cafeo, A., Gitto, E., et al. (2021). Cerebellum and prematurity: a complex interplay between disruptive and dysmaturational events. *Front. Syst. Neurosci.* 15, 655164. doi: 10.3389/fnsys.2021.655164

Steggerda, S. J., Leijser, L. M., Wiggers-de Bruine, F. T., van der Grond, J., Walther, F. J., and van Wezel-Meijler, G. (2009). Cerebellar injury in preterm infants: incidence and findings on US and MR images. *Radiology* 252, 190–199. doi: 10.1148/radiol.2521081525

Stoodley, C. J., and Limperopoulos, C. (2016). Structure-function relationships in the developing cerebellum: evidence from early-life cerebellar injury and neurodevelopmental disorders. *Semin. Fetal Neonatal Med.* 21, 356–364. doi: 10.1016/j.siny.2016.04.010

Traudt, C. M., McPherson, R. J., Studholme, C., Millen, K. J., and Juul, S. E. (2014). Systemic glycerol decreases neonatal rabbit brain and cerebellar growth independent of intraventricular hemorrhage. *Pediatr. Res.* 75, 389–394. doi: 10.1038/pr.2013.236

Tremblay, S., Pai, A., Richter, L., Vafaei, R., Potluri, P., Ellegood, J., et al. (2017). Systemic inflammation combined with neonatal cerebellar haemorrhage aggravates long-term structural and functional outcomes in a mouse model. *Brain Behav. Immun.* 66, 257–276. doi: 10.1016/j.bbi.2017.07.013

van der Heijden, M. E., Gill, J. S., and Sillitoe, R. V. (2021). Abnormal cerebellar development in autism spectrum disorders. *Dev. Neurosci.* 43, 181–190. doi: 10.1159/000515189

van der Heijden, M. E., and Sillitoe, R. V. (2021). Interactions between purkinje cells and granule cells coordinate the development of functional cerebellar circuits. *Neuroscience* 462, 4–21. doi: 10.1016/j.neuroscience.2020.06.010

Villamor-Martinez, E., Fumagalli, M., Alomar, Y. I., Passera, S., Cavallaro, G., Mosca, F., et al. (2019). Cerebellar hemorrhage in preterm infants: a meta-analysis on risk factors and neurodevelopmental outcome. *Front. Physiol.* 10:800. doi: 10.3389/fphys.2019.00800

Vinukonda, G., Hu, F., Upreti, C., Ungvari, Z., Zia, M. T., Stanton, P. K., et al. (2012). Novel organotypic in vitro slice culture model for intraventricular hemorrhage of premature infants. *J. Neurosci. Res.* 90, 2173–2182. doi: 10.1002/jnr.23102

Volpe, J. J. (2009). Cerebellum of the premature infant: rapidly developing, vulnerable, clinically important. *J. Child Neurol.* 24, 1085–1104. doi: 10.1177/0883073809338067

Wang, S. S., Kloth, A. D., and Badura, A. (2014). The cerebellum, sensitive periods, and autism. *Neuron* 83, 518–532. doi: 10.1016/j.neuron.2014.07.016

Wechsler-Reya, R. J., and Scott, M. P. (1999). Control of neuronal precursor proliferation in the cerebellum by Sonic Hedgehog. *Neuron* 22, 103–114. doi: 10.1016/S0896-6273(00)80682-0

Wei, A. D., and Ramirez, J. M. (2019). Presynaptic mechanisms and KCNQ potassium channels modulate opioid depression of respiratory drive. *Front. Physiol.* 10:1407. doi: 10.3389/fphys.2019.01407

Xue, M., Balasubramaniam, J., Buist, R. J., Peeling, J., and Del Bigio, M. R. (2003). Periventricular/intraventricular hemorrhage in neonatal mouse cerebrum. *J. Neuropathol. Exp. Neurol.* 62, 1154–1165. doi: 10.1093/jnen/62.11.1154

Yamada, K., Fukaya, M., Shibata, T., Kurihara, H., Tanaka, K., Inoue, Y., et al. (2000). Dynamic transformation of Bergmann glial fibers proceeds in correlation with dendritic outgrowth and synapse formation of cerebellar Purkinje cells. *J. Comp. Neurol.* 418, 106–120.

Yoo, J. Y., Mak, G. K., and Goldowitz, D. (2014). The effect of hemorrhage on the development of the postnatal mouse cerebellum. *Exp. Neurol.* 252, 85–94. doi: 10.1016/j.expneurol.2013.11.010

Yung, Y. C., Mutoh, T., Lin, M. E., Noguchi, K., Rivera, R. R., Choi, J. W., et al. (2011). Lysophosphatidic acid signaling may initiate fetal hydrocephalus. *Sci. Transl. Med.* 3, 99ra87. doi: 10.1126/scitranslmed.3002095

Zayek, M. M., Benjamin, J. T., Maertens, P., Trimm, R. F., Lal, C. V., and Eyal, F. G. (2012). Cerebellar hemorrhage: a major morbidity in extremely preterm infants. *J. Perinatol.* 32, 699–704. doi: 10.1038/jp.2011.185

Zhang, L., and Goldman, J. E. (1996). Developmental fates and migratory pathways of dividing progenitors in the postnatal rat cerebellum. *J. Comp. Neurol.* 370, 536–550. doi: 10.1002/(SICI)1096-9861(19960708)370:4<536::AID-CNE9>3.0.CO;2-5